

# Silica Aerogel Radiators for Bunch Length Measurements<sup>★</sup>

J. Bähr<sup>a</sup>, V. Djordjadze<sup>a</sup>, D. Lipka<sup>a,\*</sup>, A. Onuchin<sup>b</sup>,  
F. Stephan<sup>a</sup>

<sup>a</sup>*DESY Zeuthen, Platanenallee 6, 15738 Zeuthen, Germany*

<sup>b</sup>*Budker Institut of Nuclear Physics, Novosibirsk, 630090, Russia*

---

## Abstract

Cherenkov radiators based on Silica aerogel are used to measure the electron bunch length at the photo injector test facility at DESY Zeuthen (PITZ). The energy range of those electrons is 4-5 MeV. In this paper the time resolution defined by the usage of aerogel is calculated analytically and Monte Carlo simulations are performed. It is shown that Silica aerogel gives the possibility to reach a time resolution of about 0.1 ps for high photon intensities and a time resolution of about 0.02 ps can be obtained for thin Silica aerogel radiators.

*Key words:* silica aerogel, bunch length, time resolution, PITZ

---

## 1 Introduction

Successful optimization of the photo injector test facility at DESY Zeuthen (PITZ) requires beam diagnostics, allowing to measure electron beam properties with high resolution. To measure the temporal properties of electron energies of 4-5 MeV by optical means a radiation process is needed at which a photon bunch is produced with the same time properties as the electron bunch has. Optical transition radiation, which is widely used for accelerator diagnostics, produces a low number of photons per electron. In addition, those photons are produced with a wide angle distribution at these energies. Using Cherenkov radiation a significantly larger number of photons is obtained. In

---

<sup>★</sup> Partially supported by Russian Foundation for Basic Research, Grant 02-02-16321.

\* Corresponding author: dirk.lipka@desy.de

order to produce these photons in a Cherenkov cone with small opening angle a material with small index of refraction is required. Therefore, Silica aerogel is studied as alternative in this paper. For convenience of writing only the short form aerogel is mainly used hereafter.

In the following chapter the basic properties of aerogels are summarized. In chapter 3 analytical calculations on the expected degradation of the time resolution are presented. In Chapter 4 GEANT 4 simulations are compared with the analytical calculations. Finally, the results are summarized

## 2 Aerogel Radiators

### 2.1 Optical Properties

The main optical properties of aerogel [1–8] are characterized by three parameters:

- (1) Index of refraction  $n$ .

It is determined by the density  $\rho$ . The correct dependence [1] is  $n = \sqrt{1 + \alpha\rho}$  where  $\alpha = 0.438 \pm 0.001 \left(\frac{g}{cm^3}\right)^{-1}$  for a wavelength  $\lambda = 400$  nm. For low densities it is possibly to use  $n \approx 1 + k\rho$ , where  $k \approx 0.21 \left(\frac{g}{cm^3}\right)^{-1}$ . The chemical composition of aerogel is  $SiO_2$ , therefore the aerogel dispersion can be calculated from the quartz dispersion. Aerogels are produced in a range of index of refraction of 1.006 - 1.13 [1–3].

- (2) Light scattering length  $L_{sc}$ .

This quantity is defined as the path length after which a fraction  $1/e$  of the photons is not scattered. This effect is caused by Rayleigh scattering, for which  $L_{sc} \sim \lambda^4$ . Usually  $L_{sc}$  is cited at  $\lambda = 400$  nm. For good aerogel the scattering length is  $L_{sc} = 1 - 2$  cm, for best aerogels  $L_{sc} = 4 - 5$  cm. The dependence of  $L_{sc}$  on the refractive index  $n$  is weak [1,4].

- (3) Light absorption length  $L_{ab}$ .

The light absorption length is defined as the path length after which a fraction  $1/e$  of photons is not absorbed. It mainly depends on an admixture contained in the aerogel. The  $L_{ab}$  dependence on  $\lambda$  is a complicated relation [1,5]. For good aerogels  $L_{ab} = 1$  m at  $\lambda = 400$  nm and for best aerogels it reaches a value of 10 m.

## 2.2 Maximum Thickness of Aerogel

The maximum thickness of an aerogel sample is mainly limited by the scattering length  $L_{sc}$ . Lets denote the number of Cherenkov photons at unit length of the electron path by  $N_{ph,1}$ . The number of photons, which do not suffer Rayleigh scattering, in the dependence of the aerogel thickness, has a form:

$$N_{ph} = N_{ph,1} \cdot L_{sc} \cdot \left(1 - e^{-\frac{l}{L_{sc}}}\right). \quad (1)$$

The maximum number of the photons  $N_{phmax} = N_{ph,1} \cdot L_{sc}$  is reached at  $l \gg L_{sc}$ . A good choice of aerogel thickness is  $0.5 \cdot L_{sc}$ . In that case about 80 % of produced photons will be collected and 20 % will scatter. The ratio of the background to the effect is around 0.25. Therefore the maximum thickness used in this paper is  $l_{max} \approx 2$  cm.

## 2.3 Number of Photoelectrons

The number of Cherenkov photons per unit length of the particle path and per unit wavelength interval is convenient to express in the following form [9]:

$$\frac{d^2 N_{ph}}{dl \cdot d\lambda} = 2\pi \cdot \alpha \cdot \frac{1}{\lambda^2} \cdot \left(1 - \frac{1}{n^2 \beta^2}\right), \quad (2)$$

where  $\alpha = \frac{1}{137}$  and  $\beta = \frac{v}{c}$ .

Lets express a quantum efficiency of the photon detector in a form  $Q(\lambda) = Q_0 \cdot f(\lambda)$ , where  $Q_0$  is a quantum efficiency at the maximum of the spectral distribution. Lets denote the collection efficiency of the Cherenkov photons on the photo cathode of the detector by  $G(\lambda)$ . Then the photo electron number can be written as:

$$\begin{aligned} N_{pe} &= \left(1 - \frac{1}{n^2 \beta^2}\right) \cdot Q_0 \cdot l \cdot 2 \cdot \pi \cdot \alpha \cdot \int \frac{1}{\lambda^2} \cdot f(\lambda) \cdot G(\lambda) \cdot d\lambda \\ &= \left(1 - \frac{1}{n^2 \beta^2}\right) \cdot Q_0 \cdot l \cdot B(\lambda), \end{aligned} \quad (3)$$

where  $B(\lambda) = 2 \cdot \pi \cdot \alpha \cdot \int \frac{1}{\lambda^2} \cdot f(\lambda) \cdot G(\lambda) \cdot d\lambda$ .

Taking  $f(\lambda)$  for a borosilicat glass window and a bialkali photo cathode [10] with  $Q_0 = 20$  % and  $G = 1$ , particles with  $\beta = 1$  in matter with  $n = 1.5$  gives

$N_{pe} = l \cdot 65$  photo electrons, where  $l$  is the path length in cm. In Table 1 the corresponding data are presented for electrons with  $p \cdot c = 4.0$  MeV ( $\beta = 0.9919$ ) and  $p \cdot c = 4.5$  MeV ( $\beta = 0.9936$ ).

$n$	$p = 4.0$ MeV/ $c$	$p = 4.5$ MeV/ $c$
1.008	0.034	0.36
1.01	0.53	0.82
1.03	5.3	5.3
1.05	9.5	9.5
1.5	65.	65.

Table 1

Number of photo electrons per 1 cm path length of electron with  $p = 4.0$  MeV/ $c$  and  $p = 4.5$  MeV/ $c$  in materials with different index of refraction. A bialkali photo cathode with  $Q_0 = 20\%$  and a light collection efficiency of  $G = 1$  was assumed.

#### 2.4 Multiple scattering

The mean squared angle of the electron multiple scattering can be calculated using the Rossi formula including a correction [11]:

$$\theta_{MS} = \sqrt{\overline{\theta^2}} = \frac{21 \text{ MeV}}{p \cdot \beta \cdot c} \sqrt{\frac{l}{X_0}} \cdot \left( 1.0 + 0.038 \cdot \ln \frac{l}{X_0} \right). \quad (4)$$

Aerogel is  $\text{SiO}_2$ , therefore  $X_0 = 27$  g/cm<sup>2</sup>, the same as for quartz [2,11]. For refractive indices of  $n = 1.01$ ,  $n = 1.03$  and  $n = 1.05$  the corresponding radiation length is  $X_0 = 570$  cm,  $X_0 = 190$  cm and  $X_0 = 115$  cm, respectively.

In Table 2 the data for Cherenkov angle  $\theta_C$ , radius of the Cherenkov cone at the exit of the aerogel plate  $r_C = l \cdot \tan \theta_C$  and the multiple scattering angle  $\theta_{MS}$  are presented for different aerogels.

### 3 Time Resolution

#### 3.1 Reference Plane

At PITZ, the Cherenkov light will be transmitted over 26 m to the entrance slit of the streak camera by an optical transmission line. Generally, the optical system will have an influence on the time dispersion what is not considered in

$n$	1.01	1.01	1.03	1.03	1.05	1.05	1.01	1.01
$l$ , mm	20	20	2	2	1	1	2	2
$p$ , MeV/ $c$	4.0	4.5	4.0	4.5	4.0	4.5	4.0	4.5
$\theta_C$ , dg	3.5	4.8	11.8	12.3	16.2	16.6	3.5	4.8
$r_C$ , mm	1.22	1.69	0.42	0.44	0.29	0.30	0.12	0.17
$\theta_{MS}$ , dg	14.1	12.5	7.3	6.5	6.6	5.8	4.0	3.5
$\Delta_{pl}$ , ps	0.25	0.48	0.30	0.32	0.29	0.30	0.025	0.048
$\sigma_{pl}$ , ps	0.072	0.14	0.085	0.092	0.082	0.086	0.0072	0.014
$\Delta_{MS}(\delta)$ , ps	1.5	1.8	0.42	0.43	0.37	0.37	0.047	0.072
$\sigma_{MS}(\delta)$ , ps	0.45	0.51	0.12	0.13	0.11	0.11	0.014	0.021

Table 2

The parameters Cherenkov angle  $\theta_C$ , Cherenkov cone radius  $r_C$ , angle of multiple scattering  $\theta_{MS}$ , time difference because of path length differences  $\Delta_{pl}$ ,  $\sigma_{pl}$  of time difference, the time difference caused by multiple scattering  $\Delta_{MS}(\delta)$  and the corresponding  $\sigma_{MS}(\delta)$  for three aerogel radiators with  $n = 1.01$ ,  $n = 1.03$  and  $n = 1.05$  and for two incident electron momenta at different thickness  $l$ .

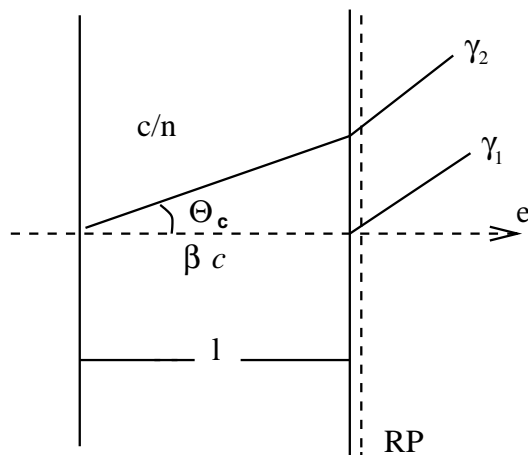


Fig. 1. Schematic view of the Cherenkov radiator system and the reference plane (RP, dashed line). The reference plane is meant to coincide with the downstream boundary of the Cherenkov radiator.

this article. To analyze the influence of the radiator itself, the streak camera entrance slit is considered to be virtually back imaged near to the exit plane of the aerogel radiator.

In this article we assume that this reference plane (RP) is located parallel to the exit plane of the aerogel (see Figure 1). All the questions concerning resolution discussed in this article are only considered up to this reference plane.

### 3.2 Thickness of Aerogel

Beside the refractive index  $n$  also the thickness of aerogel  $l$  is an important parameter for the time resolution. The optimal thickness in a real experiment has to be chosen as a compromise between two contradictory requirements. To improve the signal-to-noise ratio of the Cherenkov light detection taking into account light losses along the optical transmission line the radiator thickness has to be increased to produce more photons. But for improving the time resolution of aerogel the radiator thickness is preferred to be small, as it will be shown in the next paragraphs. Two cases are considered:

(A) Large thickness.

For comparison of aerogel samples with different  $n$  the thickness will be chosen such that the number of Cherenkov photons is equal. It means that

$$l \left( 1 - \frac{1}{n^2 \beta^2} \right) = \text{const.} \quad (5)$$

Aerogels with  $n = 1.01$ ,  $n = 1.03$ ,  $n = 1.05$  will be considered. For  $n = 1.01$  the optimal thickness is chosen to be about  $l = 20$  mm (see chapter 2.2). According to equation (5) the rounded thickness for the other radiators was chosen accordingly: for  $n = 1.03$   $l = 2$  mm and for  $n = 1.05$   $l = 1$  mm.

(B) Small thickness (for comparison).

Calculations for aerogel with  $n = 1.01$  and  $l = 2$  mm will be performed. The number of Cherenkov photons will be 10 times smaller in this case compared to case (A).

Modern technology gives the possibility to produce aerogel of such thickness.

### 3.3 Particle and Light Velocity

Electrons incident perpendicular to the aerogel plate (see Figure 1). The reference plane coincides with the second boundary of the aerogel. The time interval between the arrival of the Cherenkov photons on the reference plane is:

$$\Delta_{pl} = \frac{l \cdot n}{c \cdot \cos \theta_C} - \frac{l}{\beta c} = \frac{n^2 \beta}{c} \cdot \left( 1 - \frac{1}{n^2 \beta^2} \right) \cdot l. \quad (6)$$

This effect is caused by the time difference of the particle and light arrival at the RP plane.

For  $n = \text{const.}$   $\Delta_{pl}$  is proportional to  $l$ . This means that one can improve the time resolution by decreasing the thickness.

The time distribution of the Cherenkov photon bunch has a rectangular shape (see Figure 2, where  $t_1 = \frac{l}{\beta \cdot c}$  and  $t_2 = \frac{l \cdot n}{c \cdot \cos \theta_C}$ ), therefore the mean squared dispersion in time is  $\sigma_{pl} = \frac{\Delta_{pl}}{\sqrt{12}}$ .

The numerical values of the  $\Delta_{pl}$  and  $\sigma_{pl}$  are summarized in Table 2.

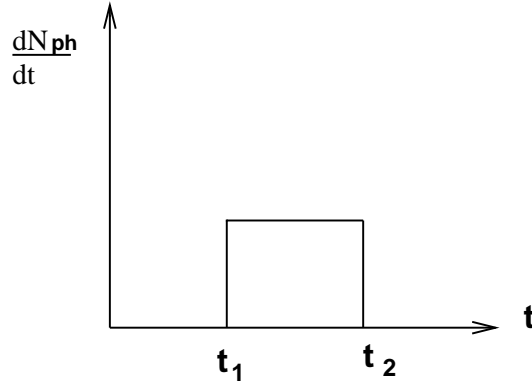


Fig. 2. Schematic view of the Cherenkov photon time distribution.

### 3.4 Dispersion of Refractive Index

To study the dependence of the time resolution on the wavelength it is convenient to write (6) in the form:

$$\Delta_{pl} = \frac{\beta l}{c} \left( n^2 - \frac{1}{\beta^2} \right) \quad (7)$$

The relative change for two different wavelengths is given by

$$\delta(\lambda_1, \lambda_2) = \frac{\Delta_{pl}(\lambda_1) - \Delta_{pl}(\lambda_2)}{\Delta_{pl}(\lambda_1)} = \frac{n^2(\lambda_1) - n^2(\lambda_2)}{n^2(\lambda_1) - \frac{1}{\beta^2}}. \quad (8)$$

One can see that  $\delta(\lambda_1, \lambda_2)$  does not depend on  $l$ . Some results of the calculation for aerogel with equation (8) are presented in Table 3 basing on quartz data from [12]. If one works far from the threshold for Cherenkov radiation  $\beta \gg 1/n$  and one uses

$$n^2 = 1 + \alpha \rho \quad (9)$$

one will receive

$$\delta(\lambda_1, \lambda_2) = \frac{\alpha(\lambda_1) - \alpha(\lambda_2)}{\alpha(\lambda_1)}. \quad (10)$$

In this case one can see that  $\delta(\lambda_1, \lambda_2)$  does not depend on  $n$  and  $l$ .

$\lambda_1$ , nm	$\lambda_2$ , nm	$\beta$	$n$		
			1.05	1.03	1.01
300	550	1	7	7	7
		0.9936*	8	9	18
		0.9919**	8	9	30
200	700	1	20	20	20
		0.9936*	23	25	40
		0.9919**	23	26	50

\* for  $p = 4.5 \text{ MeV}/c$ , \*\* for  $p = 4.0 \text{ MeV}/c$

Table 3

$\delta(\lambda_1, \lambda_2)$  in % is the relative change of  $\Delta_{pl}$  as a result of the dispersion of  $n$ .

The region  $\lambda = 300 - 550 \text{ nm}$  is the sensitive region of a bialkali photo cathode with borosilicate glass. It is seen that the dispersion is small enough for  $n = 1.05$  and  $n = 1.03$  but is 30 % for  $n = 1.01$ ,  $p = 4.0 \text{ MeV}/c$ .

The region of 200 - 700 nm is presented for a dispersion estimation as an example for a photon detector with a wider sensitivity region.

### 3.5 Transverse Beam Dimensions

The arrival time of light on the chosen plane RP does not depend on the transverse coordinates of the electron, that's why there is no dispersion connected to the transverse size of the electron beam.

### 3.6 Angular Distribution of the electron beam

Two electrons  $e_1$  and  $e_2$  cross simultaneously the plane 1 (see Figure 3). The electron  $e_1$  incidents perpendicular to the aerogel plate and electron  $e_2$  incidents by an angle  $\alpha$ . In this case the time interval of the Cherenkov photons

on the RP plane increases to

$$\Delta_\alpha = \frac{l}{c} \cdot \left( \frac{n}{\cos(\alpha + \theta_C)} - \frac{1}{\beta} \right). \quad (11)$$

A typical value of  $\alpha$  at the position where the Cherenkov radiator will be used at PITZ is  $0.1^\circ$ . The resulting contribution of  $\alpha$  to the time resolution is negligible small because  $\alpha \ll \theta_C$ .

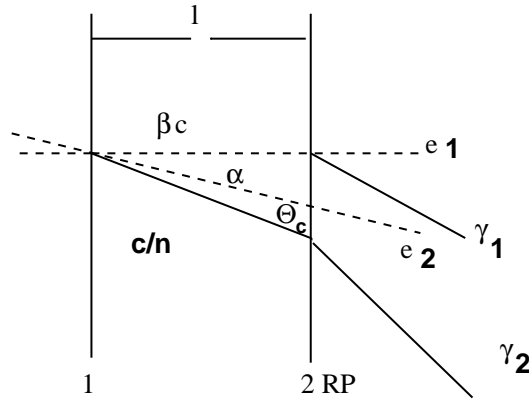


Fig. 3. Schematic view of the Cherenkov photon emission with different incident angles of the incoming electrons.

### 3.7 Multiple Scattering

Multiple scattering in aerogel creates an angular spread of the electron beam, therefore it leads to a time dispersion as given by the equation (11). The analytical calculation of this effect is complicated. One could put  $\alpha = \theta_{MS}$  in equation (11). In this case one will do an overestimation of the multiple scattering influence, because the angle  $\theta_{MS}$  refers only to the electrons at the exit of the aerogel. The photons produced in the first part inside of the aerogel will have more narrow distribution than the photons produced in the last part.

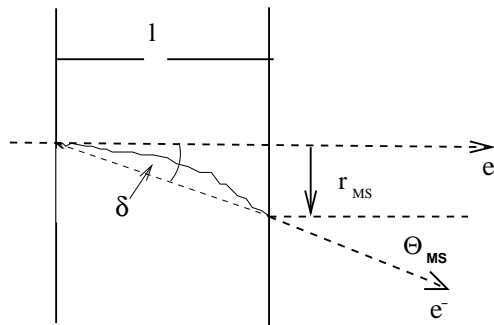


Fig. 4. Schematic view of the electron angular spread and shift due to the multiple scattering.

The mean squared value of the trajectory shift is  $r_{MS} = \frac{1}{\sqrt{3}} \cdot \theta_{MS} \cdot l$  [11] (see Figure 4). Lets introduce an angle  $\delta$ , so that  $tg\delta = \frac{r_{MS}}{l} = \frac{1}{\sqrt{3}} \cdot \theta_{MS}$  and lets assume that  $\alpha = \delta$ . The value of  $\Delta_{MS}(\delta) = \frac{l}{c} \cdot \left( \frac{n}{\cos(\delta+\theta_C)} - \frac{1}{\beta} \right)$  is presented in Table 2. It is seen that thin aerogel radiators and the use of aerogel with high index of refraction is preferred.

In Table 2 an estimation of  $\sigma_{MS}(\delta)$  which is defined as  $\sigma_{MS}(\delta) \approx \Delta_{MS}(\delta)/\sqrt{12}$  is included. For  $n = 1.05$ ,  $n = 1.03$ , and  $n = 1.01$  with  $l = 2$  mm the influence of multiple scattering is small, therefore the shape of the time spectrum is approximately rectangular. For  $n = 1.01$  with  $l = 20$  mm it is a rough estimation.

The data from Table 2 shows, that aerogel with  $n = 1.01$ ,  $l = 2$  mm gives the possibility to reach a time resolution  $\sigma_{MS}(\delta) = 0.02$  ps. Aerogel with  $n = 1.05$ ,  $l = 1$  mm gives 10 times more photons and  $\sigma_{MS}(\delta) = 0.1$  ps, whereas aerogel with  $n = 1.05$ ,  $l = 10$  mm would give 100 times more photons and  $\sigma_{MS}(\delta) = 2$  ps.

### 3.8 Other Effects

Rayleigh scattering of Cherenkov photons inside aerogel is not considered. The scattered photons would have a wide angular distribution and only a small part of them would be within the acceptance of an optical transmission line.

The effect of energy loss due to ionization and Bremsstrahlung is negligible small. Compton scattering of Cherenkov photons is much smaller than Rayleigh scattering therefore this effect gives a negligible contribution to the time resolution. Scattering of photons on the boundary of aerogel is not considered because the index of refraction is small.

## 4 Time Resolution. Monte Carlo Results

### 4.1 Simulation conditions

Simulations of the electron beam passage through aerogel for the PITZ set-up were performed using the GEANT 4 [13] code. The simulation setup consists of a vacuum tube with the electron beam, an Aluminium entrance window, the aerogel piece and the corresponding reference plane (see Figure 5). The thickness of the aerogel plate  $l$  is chosen as it is described in chapter 3.2.

Aerogel materials ( $\text{SiO}_2$ ) with index of refraction of 1.01, 1.03 and 1.05 are investigated. In front of the aerogel a  $20\ \mu\text{m}$  thick Aluminium window can be positioned. This window will be used in the experiment to protect the rest of the PITZ vacuum system from outgasing particles from aerogel. An ideal photon detector is placed behind the aerogel at the reference plane as described above (see chapter 3.1).

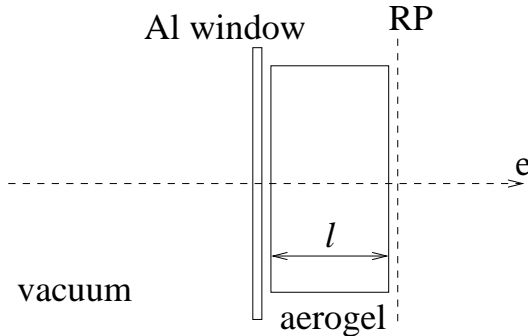


Fig. 5. Schematic view of the geometry of the GEANT 4 input.

Electrons produce Cherenkov photons inside the aerogel in a wavelength range of 350 to 800 nm. The GEANT program was configured to do a Cherenkov light simulation without wavelength dependence of the refractive index and assuming a photon detection efficiency of 100 percent. The physical processes include Cherenkov effect, Rayleigh scattering, multiple scattering, ionization and Bremsstrahlung. These processes are switched on one after another. No absorption and reflection of the Cherenkov light at the boundaries of the aerogel were considered.

#### 4.2 Acceptance model of the Optical Transmission Line

To estimate the needed acceptance of the optical transmission line behind the aerogel plate the transverse distribution of the photon emission points from the aerogel backplane and the angular distribution of the emitted photons are calculated for different processes. Both distributions are calculated with respect to the incident electron position and direction.

Figure 6 shows the distribution of the photon output angle with respect to the incident electron direction for two examples:  $n = 1.01$  and thickness  $l = 20\ \text{mm}$  (figure top) and  $n = 1.05$  and  $l = 1\ \text{mm}$  (figure bottom) for an electron momentum of  $4.5\ \text{MeV}/c$ . The processes described above are applied one after another. The Cherenkov effect alone results in an angle  $\theta_C$  equally to that shown in Table 2. By adding Rayleigh scattering an almost constant background is produced, the peak at  $\theta_C$  is still very clear. The electron scattering in the aerogel and the Aluminium window causes a smearing of the distribution and a strong increase of the tail of the distribution. The behavior

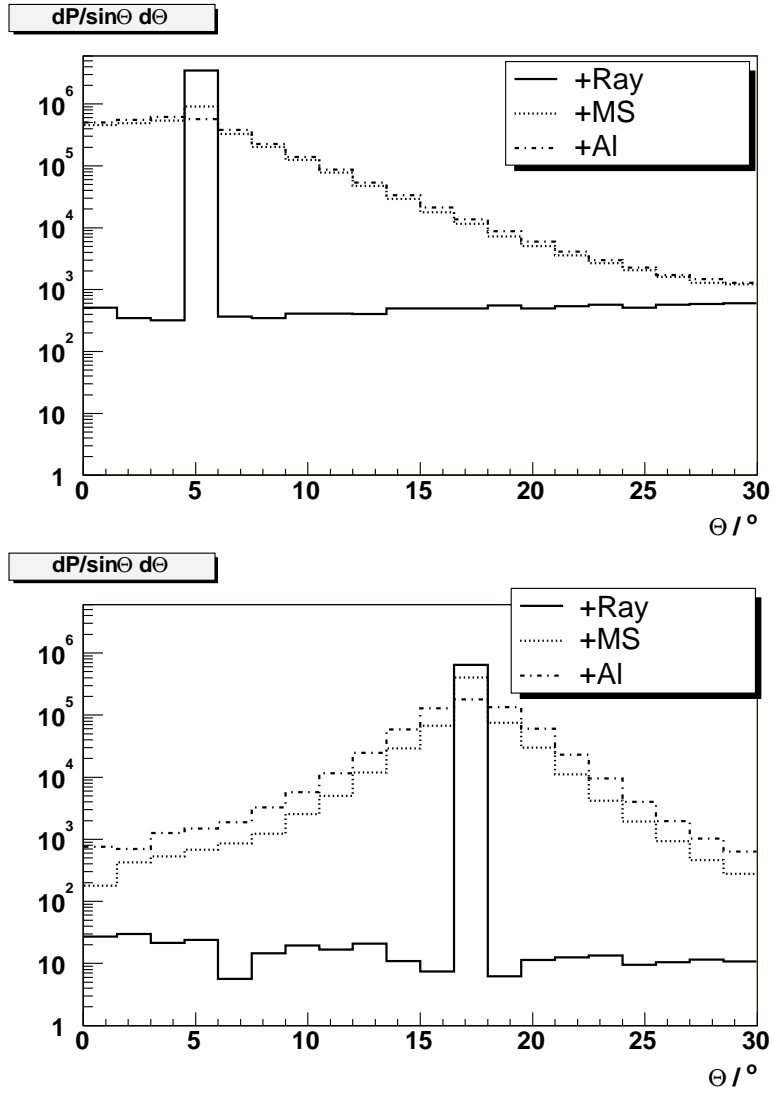


Fig. 6. Distribution of the Cherenkov photon bunches output angle with respect to the incident electron direction for  $n = 1.01$  and thickness  $l = 20 \text{ mm}$  (upper figure) and  $n = 1.05$  and  $l = 1 \text{ mm}$  (lower figure) for an electron momentum of  $4.5 \text{ MeV}/c$ . +Ray means just considering the Cherenkov effect and Rayleigh scattering. +MS means the inclusion of multiple scattering and +Al that of the Aluminium window. Here the processes are added one after another.

is similar for aerogel of different refractive indices and thicknesses except that the Cherenkov angle peak occurs at different angles.

Figure 7 shows the distribution of the photon output radius  $r$  with respect to the incident electron position for  $n = 1.01$  and thickness  $l = 20 \text{ mm}$  (upper figure) and  $n = 1.05$  and  $l = 1 \text{ mm}$  (lower figure) for an electron momentum of  $4.5 \text{ MeV}/c$ .  $r$  is the distance between the exit point of photons in the aerogel exit plane relative to the incident electron beam position. In these figures the different processes were added one after another. For the Cherenkov effect

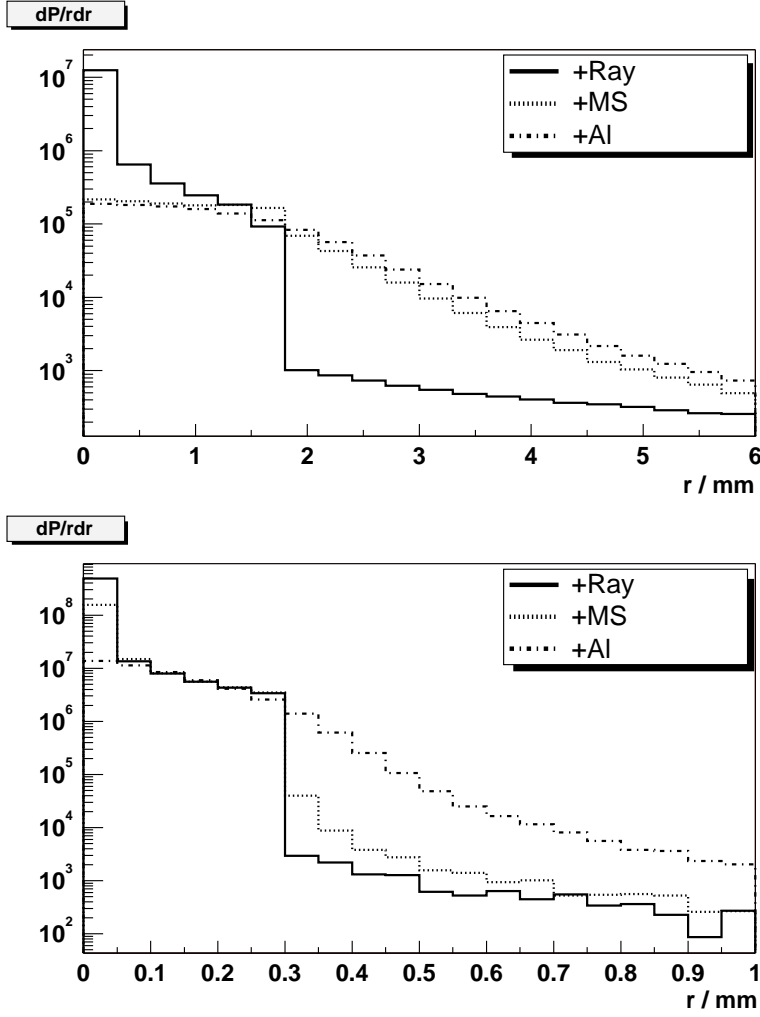


Fig. 7. Distribution of the Cherenkov photon bunches output radius with respect to the incident electron position for  $n = 1.01$  and thickness  $l = 20$  mm (upper figure) and  $n = 1.05$  and  $l = 1$  mm (lower figure) for an electron momentum of  $4.5$  MeV/ $c$ . Here the processes are added one after another. +Ray means the inclusion of Rayleigh scattering, +MS the inclusion of multiple scattering and +Al that of the Aluminium window. The calculated values of  $r_C$  for pure Cherenkov effect are  $r_C = 1.69$  mm and  $r_C = 0.30$  mm respectively.

alone a radiation intensity edge occurs corresponding to  $r_C$  as shown in Table 2. Rayleigh scattering results in photons with larger radii but small intensities. By adding multiple scattering and the Aluminium window the probability for larger radii increases and for smaller radii decreases. The effect of multiple scattering is much stronger for aerogel with low index of refraction.

For a realistic experimental design an acceptance angle for the optical transmission line between radiator and streak camera has to be chosen. Adding  $\theta_C$  and  $\theta_{MS}$  for the first three cases in Table 2 leads to a choice of an acceptance angle of about  $20^\circ$ . In addition, all photons inside of a 5 mm radius around

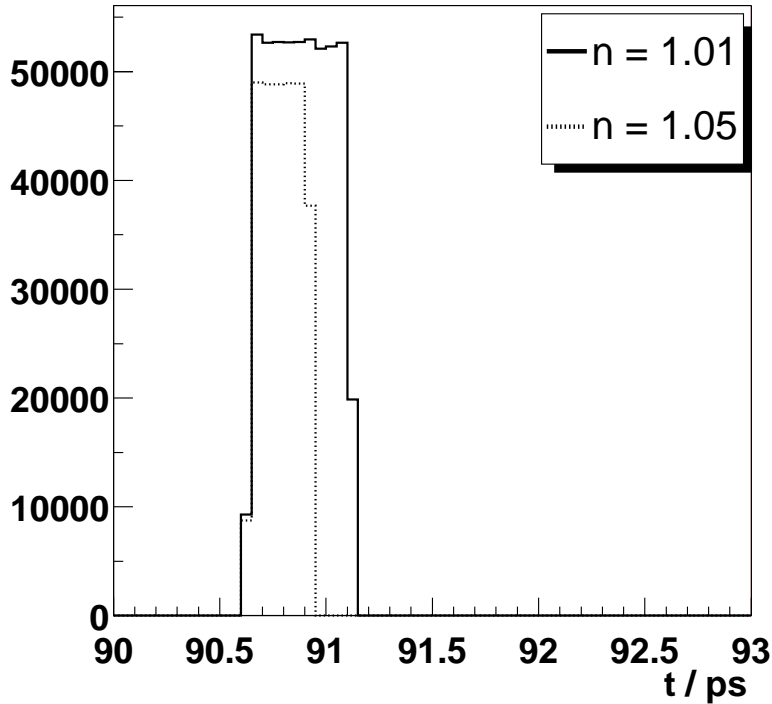


Fig. 8. Time distribution of Cherenkov photon bunches produced by electron bunches of  $4.5 \text{ MeV}/c$  momentum, fixed electron direction and point-like source, no consideration of Rayleigh scattering, multiple scattering and Aluminium window. The thickness of the aerogel samples is 20 mm for  $n = 1.01$  and 1 mm for  $n = 1.05$ .

the initial electron direction are accepted, because the typical electron beam size at PITZ is smaller than this transverse size. This choice of cuts in angle and radius includes the peaks and edges seen in the Figures 6 and 7, therefore most photons are collected. The following simulations are shown assuming these acceptance cuts.

#### 4.3 Particle and Light Velocity

To study the influence of different effects on the time resolution, simulations were performed step by step adding new phenomena to be considered in the simulation. The simplest case is when the bunch length is set to be zero and all electrons are assumed to have the same momentum, no Aluminium window is in front of the aerogel and neglecting all electron interactions except the Cherenkov radiation. The electrons incident angle is perpendicular to the aerogel plate.

Figure 8 shows the time distribution of Cherenkov photons produced by elec-

tron bunches of  $4.5 \text{ MeV}/c$  momentum and arriving at the photon receiver plane for aerogels with  $n = 1.01$  and  $n = 1.05$  within the acceptance angle. The simulation time clock starts when the electrons start to move and ends when the photons, produced by the electrons, reach the photon receiver. This time distribution has a rectangular shape as expected from Figure 2. The FWHM of these distributions is in agreement with the theoretical calculation of  $\Delta_{pl}$  (see Table 2.). The simulated Cherenkov angle  $\theta_C$  and cone radius  $r_C$  coincide with the expected values (see Figure 6 and 7).

The integral of the distribution shown in Figure 8 is proportional to the amount of emitted Cherenkov photons. These integrals are not equal for both distributions because the thickness was optimized for a momentum of  $4 \text{ MeV}/c$ .

#### 4.4 Rayleigh Scattering

To study the influence of Rayleigh scattering on the time resolution, a scattering length of  $40 \text{ mm}$  at  $400 \text{ nm}$  wavelength is assumed, using the proportionality mentioned in chapter 2.1 (2). The resulting time distributions for an electron momentum of  $4.5 \text{ MeV}/c$  are shown in Figure 9. The FWHM does not change compared to Figure 8. A small decrease of intensity with time can be observed because of a longer way of the photons inside of the aerogel compared to photons which are produced near to the reference plane. The scattered photons have a large angle and radius (see Figure 6 and 7) and therefore are mainly outside of the acceptance range.

#### 4.5 Multiple Scattering

To study the influence of multiple scattering, this process was included in the simulation. The processes ionization and Bremsstrahlung are added, too. Figure 10 shows the time distributions of photons reaching the photon receiver for an electron momentum of  $4.5 \text{ MeV}/c$ . For a refractive index of  $n = 1.01$  the shape of the distribution is changed completely compared to Figure 9, it now has a long tail. The shape for  $n = 1.05$  is mainly conserved, only for a logarithmic scale a small tail can be observed too. The reduction of the photon intensity at the beginning of the distribution compared to Figure 9 is explained by the fact that due to multiple scattering the electron direction is changed. This results in a wider angular distribution of the emitted photons yielding longer path length.

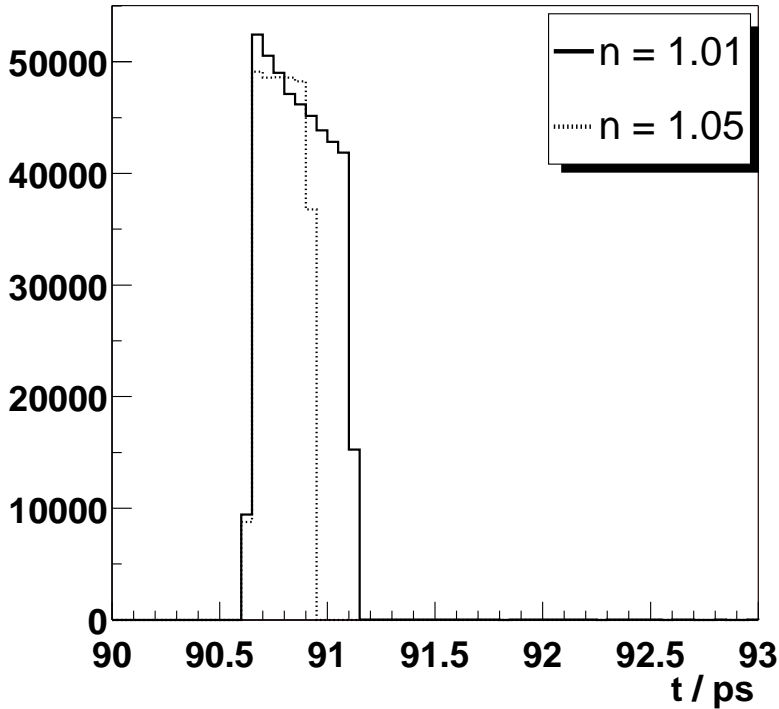


Fig. 9. Time distribution of Cherenkov photon bunches considering Rayleigh scattering produced by an electron bunch of  $4.5 \text{ MeV}/c$  momentum, without multiple scattering and Aluminium window. The thickness of the aerogel samples is 20 mm for  $n = 1.01$  and 1 mm for  $n = 1.05$ .

#### 4.6 Aluminium Window

An Aluminium window of  $20 \mu\text{m}$  thickness is placed in front of the aerogel. This causes a scattering of the electrons before they enter the aerogel. Figure 11 shows the resulting time distributions for an electron momentum of  $4.5 \text{ MeV}/c$ . The tails are increased and longer. This is significant for  $n = 1.01$ . For  $n = 1.05$  the tail is smaller by a factor of  $10^3$ . Therefore it is not visible in this linear plot.

#### 4.7 Resolution

The described time distributions are calculated assuming a point-like electron source. The *RMS* time duration is a measure of the *RMS* time resolution of the system. These values are shown in Table 4. The *RMS* values are increased and decreased with adding one effect after another. The reason is that some photons can be scattered away out of the acceptance cone and give no contribution to the *RMS* value. The last line of Table 4 is comparable with  $\sigma_{MS}(\delta)$

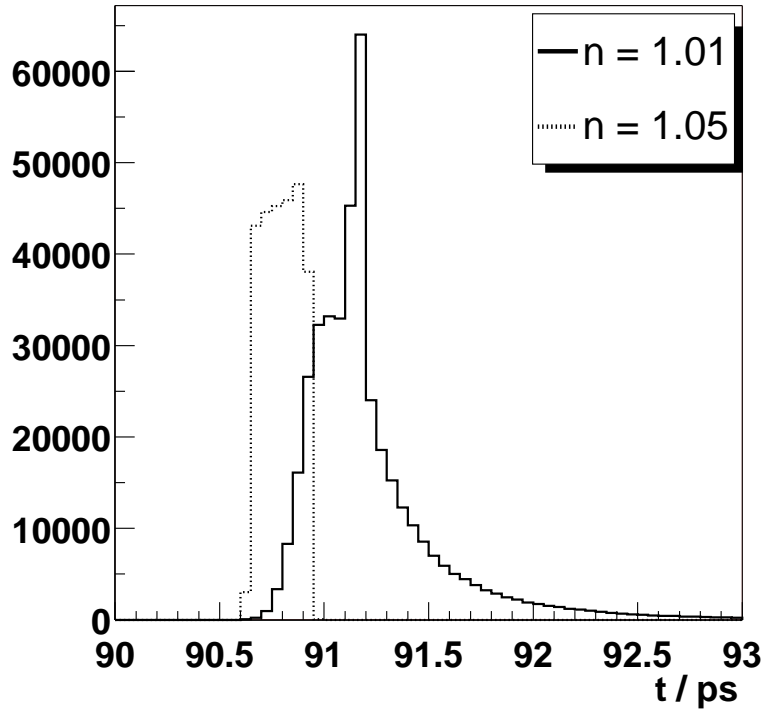


Fig. 10. Time distribution of Cherenkov photon bunches produced by electron bunches with a zero electron bunch length. Rayleigh and multiple scattering, ionization and Bremsstrahlung in aerogel are considered. No Aluminium window is used, the momentum is  $4.5 \text{ MeV}/c$ . The thickness of the aerogel samples is  $20 \text{ mm}$  for  $n = 1.01$  and  $1 \text{ mm}$  for  $n = 1.05$ .

of Table 2.

	$n = 1.01$	$n = 1.03$	$n = 1.05$	$n = 1.01$
$l, \text{ mm}$	20	2	1	2
Cherenkov	0.14	0.092	0.086	0.014
+Ray	0.60	0.104	0.090	0.014
+MS	0.80	0.094	0.084	0.012
+Al	0.58	0.110	0.091	0.017

Table 4

*RMS* time resolution in ps for different refractive indices and different thicknesses of aerogel samples for an electron momentum of  $4.5 \text{ MeV}/c$ . From top to bottom the processes are added to each other.

The refractive index 1.01 is preferred for a small acceptance angle of an optical transmission line, but due to the large thickness of  $20 \text{ mm}$  to obtain the same photon yield a worse time resolution is caused by multiple scattering. By using a smaller thickness, as it is described in chapter 3.2 (B) the number of

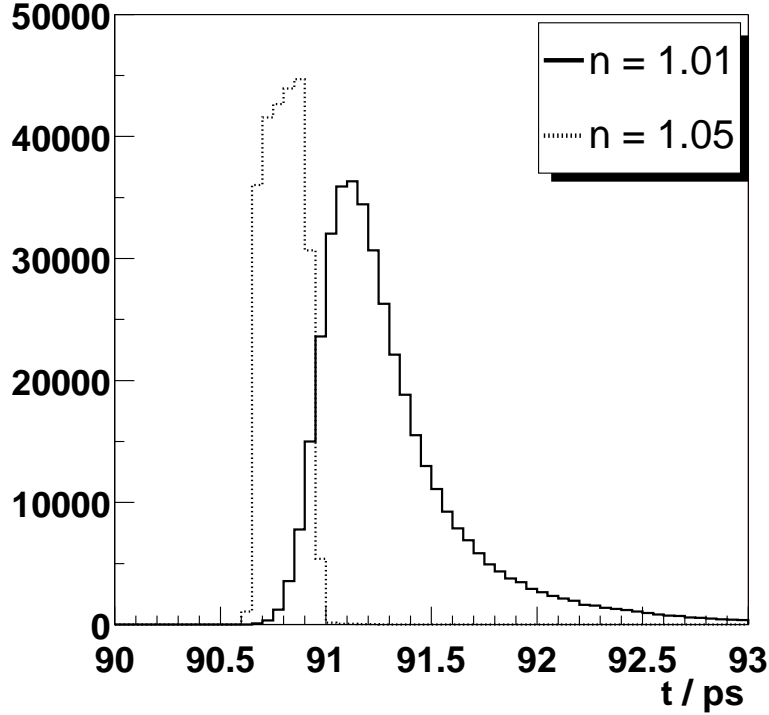


Fig. 11. Time distribution of Cherenkov photon bunches produced by electron bunches with zero electron bunch length. Rayleigh and multiple scattering, ionization and Bremsstrahlung and a  $20\ \mu\text{m}$  thick Aluminium window are considered for an electron momentum of  $4.5\ \text{MeV}/c$ . The thickness of the aerogel samples is  $20\ \text{mm}$  for  $n = 1.01$  and  $1\ \text{mm}$  for  $n = 1.05$ .

photons is decreased by a factor of 10. Figure 12 shows the time distribution for different processes, the time range is much smaller than for the thicker aerogel with  $n = 1.01$ . The corresponding time resolutions are also shown in Table 4. One can see that aerogel gives the possibility to reach a time resolution of  $0.02\ \text{ps}$ . This time resolution can be reached if the detector is able to detect the weak signal.

To determine how the proposed system will measure the bunch length distribution, an electron beam simulated with ASTRA [14] is used as input for the GEANT 4 simulation. The beam has a transverse size of  $RMS_{x,y} = 2.3\ \text{mm}$  and an angle distribution of  $RMS_{x',y'} = 1.6\ \text{mrad}$  with a mean momentum of  $4.54\ \text{MeV}/c$  and a momentum spread of  $1.4\ \%$ .

The example shown in Figure 13 is for the worst case of time resolution for  $n = 1.01$  and thickness  $l = 20\ \text{mm}$ . The thick solid line represents the time distribution of the electron beam, the thin line shows the time distribution produced by Cherenkov photons in aerogel. Only small differences can be seen. The distributions for the other considered aerogels matches even better to the electron beam temporal distribution.

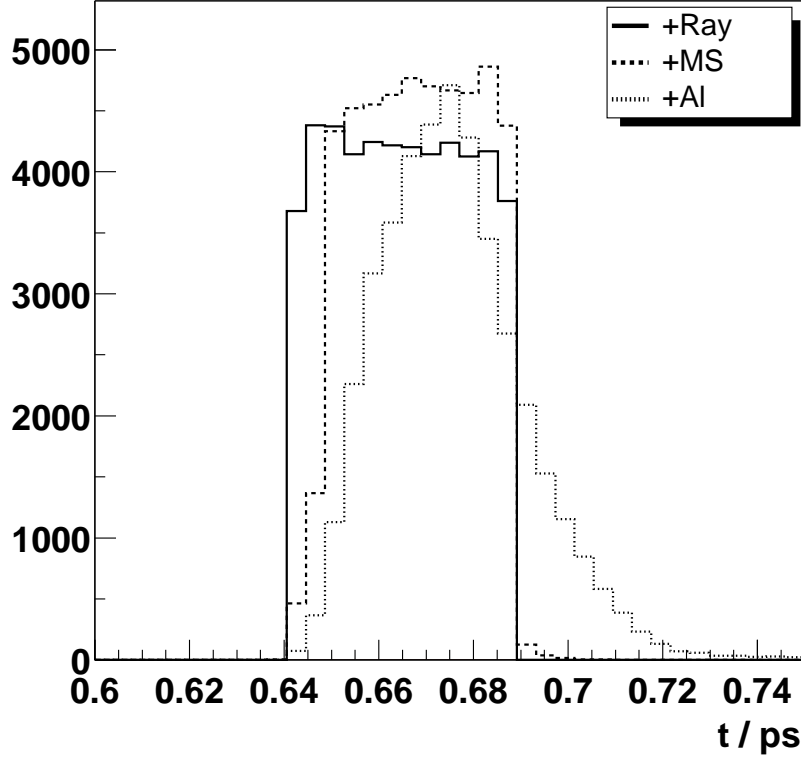


Fig. 12. Time distribution of Cherenkov photon bunches produced by electron bunches in aerogel with refractive index of 1.01 for a momentum of  $4.5 \text{ MeV}/c$  for different effects, the effects are added after another. The thickness of the aerogel sample is 2 mm.

## 5 Summary

The time resolution of aerogel radiators used for the measurement of the electron bunch length at the PITZ facility is analytically calculated and simulated with GEANT 4. It was shown, that for aerogel of refraction index  $n = 1.05$ , 1 mm thickness and an Aluminium window of  $20 \mu\text{m}$  thickness, the temporal system response has a rectangular shape with the RMS resolution of  $\sim 0.1 \text{ ps}$ . The tails are at the level of  $10^{-3}$ . Such a radiator will allow to study the bunch structure of the electrons. In addition, it is shown that with aerogel of  $n = 1.01$  and 2 mm thickness a time resolution of  $\sim 0.02 \text{ ps}$  could be reached if photon detectors with a corresponding time resolution and sensitivity would be available.

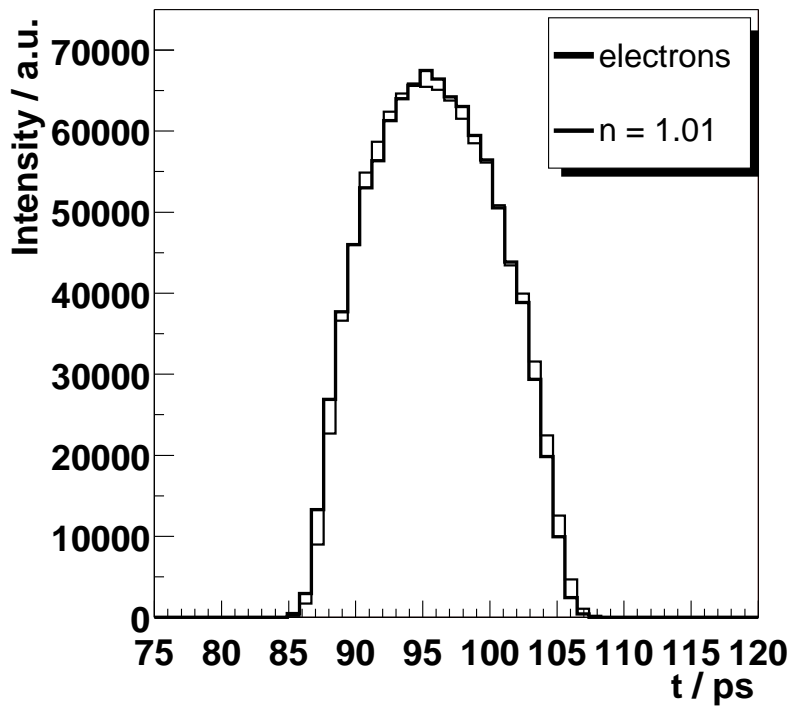


Fig. 13. Time distribution of an simulated electron beam and its corresponding Cherenkov photon beam produced in aerogel (refractive index  $n = 1.01$ , thickness 20 mm). The distributions are normalized to their areas.

## 6 Acknowledgments

We would like to thank A. F. Danilyuk, S. A. Kononov, E. A. Kravchenko and P. V. Logachev for the fruitful discussion.

## References

- [1] A. F. Danyliuk et al., Nucl. Instr. and Meth. A 494 (2002) 491.
- [2] A. R. Buzykaev et al., Nucl. Instr. and Meth. A 433 (1999) 396.
- [3] T. Iijima et al., Nucl. Instr. and Meth. A 453 (2000) 255.
- [4] A. R. Buzykaev et al., Nucl. Instr. and Meth. A 379 (1996) 465.
- [5] M. Yu. Barnyakov et al., Nucl. Instr. and Meth. A 453 (2000) 326.
- [6] A. F. Danyliuk et al., Nucl. Instr. and Meth. A 433 (1999) 406.
- [7] M. Yu. Barnyakov et al., Nucl. Instr. and Meth. A 494 (2002) 424.

- [8] T. Iijima et al., Tests of a proximity focusing RICH with aerogel as radiator, talk presented at RICH 2002, to be published at Nucl. Instr. and Meth.
- [9] I. M. Frank, I. E. Tamm, Dokl. Akad. Nauk, SSSR (1937) 14(3) 109.
- [10] 'Photomultiplier Tubes', Catalog TPM0003E02, Hamamatsu, Oct. 1998 T. (1998)
- [11] K. Hagiwara et al., Particle Data Group, Physical Review D66, 010001 (2002)
- [12] F. Kohlrausch, Teubner Verlag, ISBN 3-519-23000-3 (1996)
- [13] GEANT 4, <http://wwwinfo.cern.ch/asd/geant4/geant4.html>
- [14] K. Flöttmann, "A Space Charge Tracking Algorithm",  
<http://www.desy.de/~mpyflo/>.